

# Evaluation of Photodetectors for the Photoplethysmographic Signal Detection of Hand Epidermal Layer



Celeste M. Ojeda<sup>1</sup>, Glenn G. Fabia<sup>2</sup>, Jennifer C. Dela Cruz<sup>3</sup>

<sup>1</sup>Graduate Studies, Mapua University

<sup>1</sup>Electronics and Computer Engineering Department, Ateneo De Naga University

<sup>2</sup>Computer Science Department, Ateneo De Naga University

<sup>3</sup>School of EECE, Mapua University

## ABSTRACT

This study presents the potential of using photoplethysmography (PPG) as an alternative to the use of expensive spectroscopy or invasive skin biopsy to analyse skin conditions, particularly of the presence or absence of melanin in both dorsal and palmar skin of human subjects. This study seeks to analyse the sensing capabilities of three photodetectors (phototransistor, light dependent resistor, photodiode) vis-à-vis varying LED colors and quantities using backscatter radiation. Further, it intends to distinguish the best detector and LED color-quantity combination for the sensing of PPG signal in both dorsal and palmar skin of human volunteers. Photoplethysmography (PPG) is considered as a facile and cost effective optical process frequently used for monitoring heart rate. A light source or emitter and a light sensor or detector make up a PPG circuit. A light emitting diode (LED) is the frequently used light source while phototransistor, photodiode or light dependent resistor are the usual light sensors or detector employed. The simulation results revealed that four pieces of yellow LED and phototransistor detector are the best combination for applications involving the melanin in dorsal and palmar skin. The results further showed direct proportionality relationship between reflected light and age.

**Key Words :** backscatter radiation, photodetectors, photoplethysmography, reflectance

## 1. INTRODUCTION

Photoplethysmography (PPG) is a facile and cost effective optical[1] process frequently used for monitoring heart rate[2]. The measurement is usually done at the surface of the skin[3] with a light source and photodetector or sensor. As early as the 1930's, PPG application was already employed in blood volume measurements[4] where a variation in light was likewise seen as a variation in blood volume. The method, thus, employed the Light Absorption and Reflection Principle and this similar concept was applied in this study; but, human skin color was considered instead of the usual blood volume changes. Particularly, the dorsal and palmar skin areas were assessed. These areas were considered due to obvious color differences particularly skin Type V-VI of the Fitzpatrick scale[5]. A darker skin meant a greater amount of melanin[6] present and therefore, more light absorption was likely to follow. Melanin,

Light source or emitter and light detector or sensor[8] comprise the PPG circuit. The usual light source used is the light-emitting diode (LED); while the common light sensors employed are photodiode, light-dependent resistor (LDR), or phototransistor.

At present, several types of research on PPG have been done which extracted information on other applications apart from heart rate estimation and the likes[2]. These include stenosis vessel analysis after hemodialysis process [9], blood-oxygen-level measurement[10], blood flow analysis as indicator of blood pressure [11], blood volume changes [12], arterial condition analysis for diabetics[13], measurement of deviations in oxygen saturation[14], [15], [16] analysis of sleep staging phase[17], vital signs detection[18], heart rate measurement during bike activity[19], pulse volume estimation[20], blood pressure monitoring while sleeping[21], drowsiness assessment[22], blood flow estimation in the carotid artery[23], arterial oxygen saturation[24], to name some. All these involved PPG circuits being connected to body parts where information is desired and without any discomfort felt by the patient [25]. Presently, PPG signals have been tested as wearable electronic devices[10], as well as contactless[26] or remote PPG (rPPG)[3]. The latter means utilizing facial videos to create signals[27], [28], [29].

Different conditions for both light source and detector are considered for different PPG information. Apart from the source to area distance, the number of light sources must also be considered. Through the use of a PPG circuit in this study, the number, as well as the color, of the light source to be used had been examined. Generally, it aims to verify the leading probable combination of source color-quantity and sensor that would provide the best PPG response. Particularly, it aims to (1) ascertain the best LED color and its corresponding wavelength for the recognition of PPG signal in the dorsal and palmar skin of volunteers; (2) identify the number of LED to be used for best PPG signal detection in the specified skin of volunteers or participants and; (3) distinguish the best light sensor or detector for PPG signal detection in the dorsal and palmar skin of volunteers. This study used yellow, red, and orange[30] LEDs, with wavelengths at 590 nm, 630-640 nm, 610 nm, respectively, as the light sources where the detection of PPG signal was observed by altering its quantity. Considering the specific wavelength of each LED source used, its depth of penetration[31] plays an imperative function in the

measurement of the desired signal. In this study, the melanin present in the dorsal and palmar skin was the desired component to be measured.

Phototransistor, LDR, and photodiode were the light sensors or detectors used. Before testing, participants were made to sign a Consent Form. And during the testing, gender and age were considered because of two reasons, namely: (1) females have a lighter complexion than similar-aged males[32] which meant lesser melanin present; (2) the quantity of melanocyte, the melanin-producing cell, is said to decrease by 8 to 20% per decade after the age of 30 in both sun-exposed and unexposed areas of the skin[33].

## 2. MATERIALS AND METHODS

This study involved testing different quantities of yellow, orange, and red [30] LED sources vis-à-vis phototransistor, LDR, and photodiode. The principle followed was Backscatter Radiation which utilized the rebound of photons taking place from light source to measured area to photosensor. The amount of reflected light reaching the different light sensors[34] would, therefore, be measured. Particularly, it targets to define the best combination of source color-quantity and sensor that would provide the best PPG response. A distance of 2-3 cm from the light source to the measured skin was observed. Twelve persons participated in the testing with the following profile: (1) one 10-year old boy with type III skin in the Fitzpatrick scale, labeled as 6b in the succeeding graphs; (2) one *Type IV* 5-year old girl, as 6g; (3) one *Type IV* 14-year old boy, as 5b; (4) one *Type III* 19-year old girl, as 5g; (5) one *Type IV* 23-year old man, as 4b; (6) one *Type IV* 23-year old woman, as 4g; (7) one *Type IV* 35-year old man, as 3b; (8) one *Type IV* 35-year old woman, as 3g; (9) one *Type III* 41-year old man, as 2b; (10) one *Type III* 41-year old woman, as 2g; (11) one *Type IV* 52-year old man, as 1b; and (12) one *Type III* 54-year old woman, as 1g.

A short briefing regarding the study, its objectives and the testing areas, were discussed to the participants. A Participant's Consent Form was signed prior to testing. For the three minor participants (10-year old boy, 5-year old girl, and 14-year old boy), a guardian's permission was also requested. The dorsal skin was tested first, then the palmar skin.

Figure 1 shows the basic circuit with the following compositions: (1) light sources; (2) light sensors; (3) bar graph indicator; (4) DC to DC converter; (5) ATmega328 microcontroller.

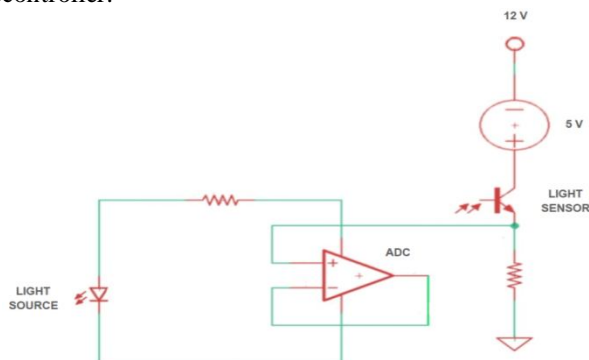


Fig. 1. Basic PPG Circuit

The light source in Figure 1 refers to the three different LEDs that were used separately. The wavelengths of the LED were specified at 630-640 nm, 610 nm, and 590 nm for red, orange, and yellow, respectively. The first part involved testing one piece of LED color versus phototransistor then LDR and last photodiode. Next, two pieces were tested, then three and last was four pieces. Figure 2 shows the LED light assembly. The light assembly, in the figure, is composed of four LEDs.

The light sensor, still in Figure 1, refers to the three different light sensors or detectors, particularly the phototransistor, LDR, and photodiode. Figure 3 shows the encapsulated sensors used in this study.

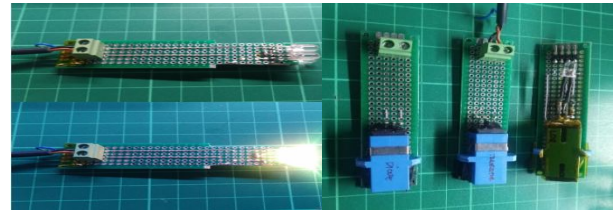


Fig. 2. LED Light Assembly

Fig. 3. Encapsulated Sensors Used

Figure 4 shows the actual circuit with the third component of the PPG circuit, that is the bar graph indicator. As shown in the figure, the bar graph indicator represents the digital output signature of the photodetectors. It is comprised of ten ordinary LEDs that lit when a signal was identified. In Figure 1, 5V was supplied to the light sensor, so lit LED in the bar graph indicator meant a sensor output of 500 mV. This output was likewise the input to the microcontroller. A 10-lit LED in the bar graph indicator meant a detected output of 5V. The fourth and fifth components are the DC to DC converter and ATmega328 Module, respectively. The main function of the DC to DC converter was to supply limited current through the LED. This was achieved through changing current and unchanging voltage. ATmega328 Module was the microcontroller used.

Figure 4 shows the actual circuit used with the five PPG components; while, Figure 5 shows the test set-up. In the test set-up, the dorsal skin test could also be seen. Two testers (light meter and voltmeter) could also be seen in Figure 5. An aluminum anodized vertical stand was used.



Fig. 4. Actual Circuit



Fig. 5. Test Set-up

### 3. THEORY/CALCULATION

Because the palmar and dorsal skin areas were the areas involved in the testing, only the stratum basale layer of the epidermis was assessed. Epidermis, considered as the outmost skin cover, has a thickness of around 0.027 to 0.15 mm[35] and made up of four to five layers[36]. When an incident light hits the skin, three instances are likely to occur, that is reflection, absorption and scattering. Majority of the incident or transmitted light will be absorbed or scattered [37], [38] and only an approximate of 5-7% will be reflected back. The absorption that happens in the epidermis layer is primarily related to the volume of melanin present [37]. Higher absorption will occur with higher melanin concentration. A higher absorption will likewise mean lesser reflected light. Light Reflection and Absorption Principle [39] was therefore adopted in this research. This reflected light was the signal obtained by the photodetectors (phototransistor, LDR, and photodiode).

### 4. RESULTS AND DISCUSSION

For all the testings performed, the distance of the LED light source was 2-3 cm. Lit LEDs in the bar graph indicator signified a sensed output voltage. Figures 6 to 13 show the bar graph response of the three different-colored LEDs with varying quantities and with different sensors used. Though tested separately, the comparison of the response of yellow, orange, and red sources versus the different photodetectors used was shown in one figure.

Figure 6 shows the dorsal responses of the three photodetectors tested in a one-piece yellow, orange, and red LED source at a 2-3 cm distance away from the skin to be measured.

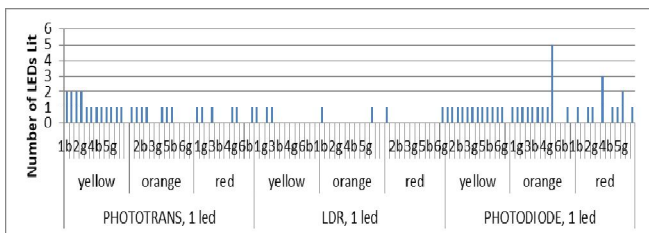


**Fig. 6.** Dorsal Response of photodetectors in 1 LED

The leftmost part of Figure 6 shows the dorsal responses of a phototransistor. As evident in the figure, the one-piece yellow LED was able to detect the dorsal skin in every human subject making it the best source than the orange and red LED sources. The center graph of Figure 6 shows the dorsal response of an LDR which demonstrated yellow LED as the best source to be utilized with an LDR sensor. The rightmost graph of Figure 6 shows the photodiode response. As can be seen, the yellow LED source was also able to provide a one-lit LED in the bar graph indicator in all sequences. With all instances detected, the yellow LED still appeared as the best source to be used with a photodiode in determining the dorsal skin response of participants.

Also in Figure 6, the yellow LED could be seen as the source to offer the greatest response in all three sensors. This is evidenced by LEDs lit in the bar graph response in all instances or every human subject tested, except in LDR. Apart from the greatest number of detected responses, the yellow LED source also gave the most regular detection pattern than the orange and red LEDs. The phototransistor sensor also gave the best response as seen in the leftmost part of Figure 6 where the gradual changes in the readings were based on the ages of the human subjects. The combination of one-yellow LED and phototransistor proved the best response in this first testing. In the next graph, Figure 7 shows the optical dorsal responses of the phototransistor, LDR, and photodiode were likewise tested in two-piece yellow, orange, and red LED sources.

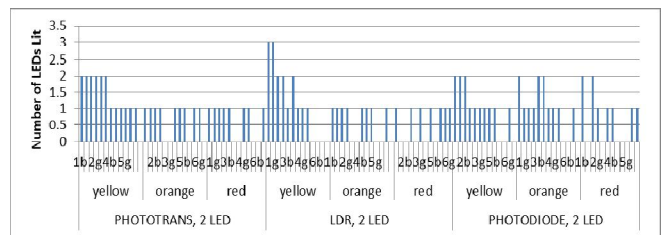


**Fig. 7.** Dorsal Response of photodetectors in 2 LEDs

In the leftmost graph of Figure 7, the dorsal bar graph responses of a phototransistor were compared. From the graph, the yellow LED offered the best phototransistor response with lit-LEDs in the bar graph indicator at all instances. Due to the greatest number of detection, the leftmost graph of Figure 7 proves that the yellow LED is the best LED source. The LDR were likewise shown in the middle graph of Figure 7. The greatest number of lit LEDs in the bar graph response of a yellow LED proves that yellow is also the best LED source for the LDR response in the dorsal skin. For the photodiode, responses were evaluated in the rightmost graph of Figure 7. Here, the yellow LED proved to be the best source compared to orange and red LEDs for the photodiode dorsal skin detection of human subjects.

Also from Figure 7, the two-piece yellow LED again offered the greatest response in all three sensors. This is evidenced by LEDs lit in the bar graph response in all instances or every human subject testing. Phototransistor also offered the greatest optical response as evidenced by the highest number of dorsal skin detection. In this two-LED testing, yellow LED and phototransistor gave the best response.

Between the one-yellow and two-yellow LEDs, the latter offered a better dorsal response to phototransistor sensors. This is demonstrated by the greater number of two-lit LEDs in the bar graph response. The two-yellow LED sources caused two LEDs to light in six instances, as shown in Figure 7, as compared to only four instances in a one-yellow LED in Figure 6. The following Figure 8 shows the dorsal responses of the phototransistor, LDR, and photodiode in three-piece yellow, orange, and red LEDs.

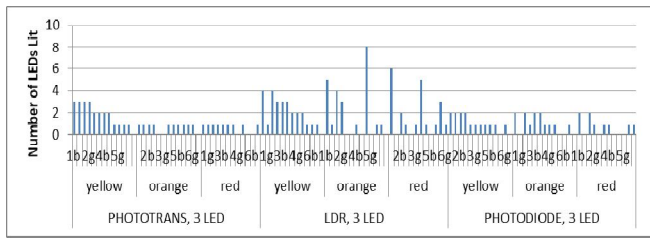


**Fig. 8.** Dorsal Response of photodetectors in 3 LEDs

The rightmost graph of Figure 8 shows the dorsal bar graph responses of a phototransistor. Here, the yellow LED offered the greatest phototransistor response as evidenced by the lit LEDs in all instances, plus, a gradual decrease in the number of lit LEDs was observed as the age of human subjects increased. In the center graph of Figure 8, the dorsal responses of LDR were tested. Here, the yellow LED also proved to offer the greatest LDR response because of two reasons, namely: (1) it had lit LEDs in all twelve instances; (2) it had the least variation in the bar graph response, in comparison to orange and red that with observed irregularities in its responses. For the photodiode response in the rightmost graph of Figure 8, yellow LEDs again offered the best photodiode response in the detection of the dorsal skin. As could be observed in this part, though not all instances were lit, it still had the most number of lit LEDs in the bar graph indicator. A gradual decrease in lit LEDs was observed in a yellow source, in contrast to an abrupt change in both orange and red sources.

In the three graphs of Figure 8, the three-piece yellow LED again offered the greatest response in all three sensors. This is evidenced by LEDs lit in the bar graph response in all instances or in every human subject tested, except in the photodiode graph which missed one instance. Among the light sensors, phototransistors also offered the greatest optical response evidenced by the highest number of dorsal skin detection. In this three-LED testing, the yellow LED and phototransistor gave the best response.

Between a two-yellow and three-yellow LEDs, a better dorsal response was seen in the three-yellow LED than the two-yellow LED. This was demonstrated by the greater number of three-lit LEDs in the bar graph response, as shown in Figure 8, in comparison to a maximum of two-lit LEDs in the bar graph indicator in a two-yellow, LED source, as shown in Figure 7.

Figure 9 shows the optical responses of the phototransistor, LDR and photodiode in four-piece yellow, orange, and red LED sources.

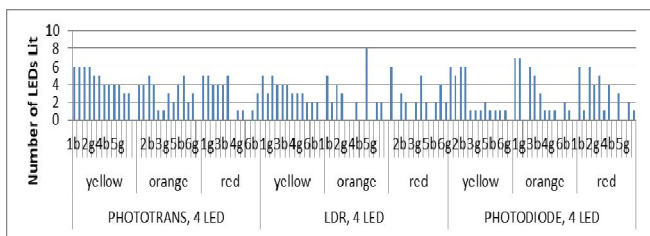


**Fig. 9.** Dorsal Response of photodetectors in 4 LEDs

In the leftmost part of Figure 9, the dorsal bar graph responses of a phototransistor were differentiated. From the graph, the yellow LED offered the best phototransistor response with lit-

LEDs in the bar graph indicator at all instances, plus, a regular decrease in the number of lit LEDs was observed as the age of human subjects increased. The orange LED also had all LEDs in the bar graph indicator to light; however, an irregular response was detected. In the center graph of Figure 9, the optical response of LDR was determined. In this part, the yellow LED offered the greatest LDR response because of two reasons: (1) it had lit LEDs in all twelve instances; (2) it had the least variation in the bar graph response compared to orange and red with observed irregularities in its responses. In the rightmost part of Figure 9, photodiode response showed that yellow LED source also had the highest number of lit LEDs. An almost gradual decrease in lit LEDs was observed in a yellow source, in contrast to an abrupt change in both orange and red sources.

From Figure 9, the four-piece yellow LED offered the greatest response in all three sensors. This is demonstrated by LEDs lit in the bar graph response in all instances or every human subject tested and in all three light sensors used. Among the light sensors, phototransistors also offered the greatest optical response as evidenced by the gradual decrease in dorsal detection. In this four-LED testing, the combination of yellow LED and phototransistor gave the best response.

Among the LED source quantities, the four-yellow LED gave the best dorsal response to a phototransistor sensor. This was demonstrated by the greater number of six-lit LEDs in the bar graph response, as shown in Figure 9, in comparison to a maximum of three-lit LEDs in the bar graph indicator in a three-yellow, LED source, as shown in Figure 8.

Figures 10 to 13 show the palmar responses of LED sources and light sensors. Similarly, though tested separately, the comparison of the response of the three sources was shown in one graph. The leftmost part of Figure 10 shows the palmar responses of a phototransistor. As can be seen, the one-piece yellow LED detected the palmar skin in every human subject testing making it the best source. A regular detection pattern could also be observed in a yellow LED, as compared to red and orange.

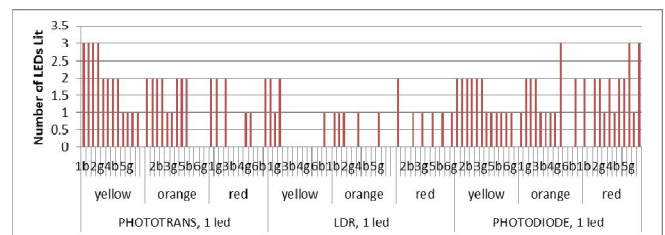


**Fig. 10.** Palmar Response of photodetectors in 1 LED

The center graph of Figure 10 shows the palmar response of an LDR. Though the three-different colored LED sources were able to detect the palmar skin in different instances, the detection pattern of the LDR from all LED sources showed a very irregular pattern making an unreliable response. The photodiode response was shown in the rightmost graph of Figure 10. With all instances detected and with a regular detection pattern, the yellow LED still appeared as the best source to be used with a photodiode in determining the palmar skin response of participants.

Figure 10 also shows yellow LED as the source to offer the greatest response as evidenced by LEDs lit in all instances or every human subject tested in a phototransistor and photodiode. The phototransistor also gave the best response as seen in the leftmost part of the figure where the gradual change in the readings were based on the ages of the human subjects. The combination of one-yellow LED and phototransistor proved the best response in this first palmar testing.

Figure 11 shows the optical palmar responses of the phototransistor, LDR, and photodiode tested in two-piece yellow, orange, and red LED sources.

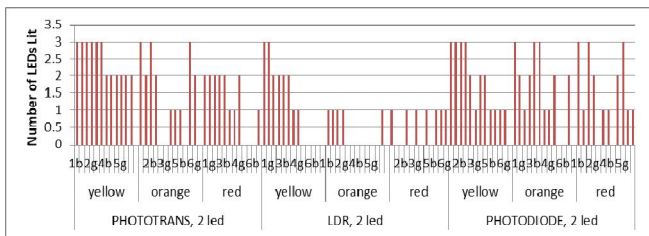


**Fig. 11.** Palmar Response of photodetectors in 2 LEDs

In the leftmost part of Figure 11, the palmar responses of a phototransistor were compared. Here, the yellow LED offered the best phototransistor response with lit-LEDs in the bar graph indicator at all instances. Due to the greatest number of detection and a regular pattern of detection, the leftmost graph of Figure 11 proves that the yellow LED is the best LED source for the phototransistor response in the palmar area. For the LDR response, the greatest number of lit LEDs of a yellow LED proves that yellow is also the best source. In the rightmost graph of Figure 11, the photodiode responses were evaluated where the complete detection of the yellow LED in all instances proved it to be the best source.

Figure 11 further shows that the two-piece yellow LED again offered the greatest response in all three sensors. This is evidenced by LEDs lit in the bar graph response in all instances or every human subject testing. Phototransistors also offered the greatest optical response as evidenced by the highest number of palmar skin detection. In this two-LED testing, the yellow LED and phototransistor gave the best response as evidenced by the complete detection during human testing and a regular response pattern.

Figures 10 and 11 both show a regular detection pattern for one-yellow and two-yellow LEDs, respectively. However, the two-yellow LED offered a better palmar response to the phototransistor sensor as demonstrated by the greater number of three-lit LEDs in the bar graph response. The two-yellow LED sources caused two LEDs to light in six instances, as shown in Figure 11, as compared to only four instances in a one-yellow LED in Figure 10.

Figure 12 shows the palmar responses of the phototransistor, LDR, and photodiode in three-piece yellow, orange, and red LEDs.

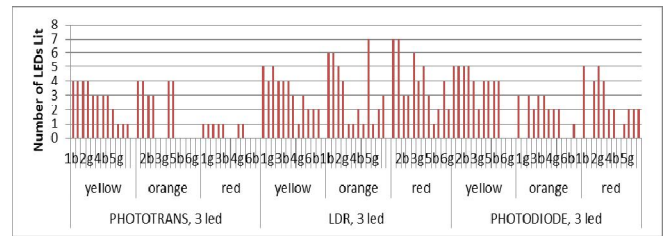


**Fig. 12.** Palmar Response of photodetectors in 3 LEDs

In the first graph of Figure 12, the palmar bar graph responses of a phototransistor were compared. In this graph, the yellow LED offered the greatest phototransistor response as evidenced by the lit LEDs in all instances, plus, a gradual decrease in the number of lit LEDs was observed as the age of human subjects increased. In the center graph, though no regular pattern was seen in the three LED sources, the yellow LED still proved to offer the greatest LDR response because it had the least variation in comparison to orange and red with obvious irregularities in its responses. In the rightmost part of Figure 12, yellow LEDs offered the best photodiode response in the detection of the palmar skin with an almost regular pattern, as opposed to the contrasting response patterns in orange and red LEDs.

Also, Figure 12 shows that the three-piece yellow LED again offered the greatest response in all three sensors. This is evidenced by the highest number of LEDs lit in the bar graph responses. Among the light sensors, phototransistors also offered the greatest optical response as evidenced by the regular detection pattern. In this three-LED testing, the yellow LED and phototransistor gave the best response.

Between the two-yellow and three-yellow LEDs, a better palmar response was seen in the three-yellow LED due to the greater number of lit LEDs in the bar graph response. A maximum of four-lit LEDs was observed in Figure 12, in comparison to a maximum of three-lit LEDs in the bar graph indicator in a two-yellow, LED source, as shown in Figure 11. The succeeding Figure 13 shows the optical responses of the phototransistor, LDR, and photodiode were tested in four-piece yellow, orange, and red LED sources.

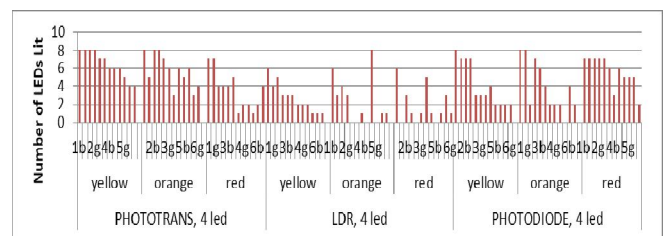


**Fig. 13.** Palmar Response of photodetector and 4 LEDs

The leftmost part of Figure 13 shows the palmar responses of a phototransistor. All LED sources caused LED in the bar graph indicator to light in all instances; however, the yellow LED offered the greatest phototransistor response as evidenced by the regular response pattern. This regular decrease in the number of lit LEDs was observed as the age of human subjects increased. The orange and red LED sources also caused all LEDs in the bar graph indicator to light; however, an irregular response was detected. In the center graph of Figure 13, the

palmar responses of LDR were seen. Here, the yellow LED proved to offer the greatest LDR response because of two reasons, namely: (1) it had lit LEDs in all twelve instances; (2) it had the least variation in the bar graph response. The photodiode response is shown in the rightmost graph. As seen, both yellow and red LED sources completely detected all instances as evidenced by the full detection in the bar graph indicator; but, the yellow LED displayed an almost regular pattern than the red LED source. An almost gradual decrease in lit LEDs was observed in a yellow source, in contrast to an abrupt change in both orange and red sources.

From Figure 13, the four-piece yellow LED again offered the greatest response in all three sensors. This is demonstrated by LEDs lit in the bar graph response in all instances or every human subject tested and in all three light sensors used. Among the light sensors, phototransistors offered the greatest optical response as evidenced by the gradual decrease in palmar detection. In this four-LED testing, the combination of yellow LED and phototransistor gave the best response.

Among the LED source quantities, the four-yellow LED gave the best dorsal and palmar responses to phototransistor sensors. This was demonstrated by the lit LEDs and regular response pattern in all tests conducted, as shown in the leftmost part of Figures 6, 7, 8, 9, 10, 11, 12, and 13. As could also be observed, a higher number of lit-LEDs in the bar graph indicator appeared in the palmar testing as compared to its dorsal equivalent. For example in the one-yellow LED testing of palmar and dorsal skin. A maximum of two-lit LEDs in the bar graph indicator appeared at four instances in the dorsal testing in Figure 6, in comparison to three-lit LEDs at four instances in the palmar testing at Figure 10. In the two-piece yellow LED dorsal and palmar testing in Figures 7 and 11, respectively, a maximum of two-lit LEDs were observed in the dorsal test in Figure 7; while a maximum of three-lit LEDs was observed in the palmar test in Figure 11. Such was also the case in three-piece yellow LEDs. A maximum of three-lit LEDs in the bar graph indicator was observed in the dorsal testing in Figure 8; while four-lit LEDs occurred in the palmar testing in Figure 12. In the four-yellow LED, six-lit LEDs were observed during the dorsal testing in Figure 9; but eight-lit LEDs in the bar graph indicator appeared during the palmar testing in Figure 13.

The skin's light reflectance ability was demonstrated in this study. The findings of higher lit-LEDs in the palmar than the dorsal reinforced the greater number of melanin present in the dorsal area [5]. These greater numbers of melanin absorbed the incident light; thus, causing lesser light to be reflected and be sensed by the photosensor. The results further proved the possibility of using it for assessing a person's melanin instead of spectrophotometry or skin biopsy[40].

## 5. CONCLUSION

The series of tests demonstrated that a 590 nm yellow LED had the highest sensor response to photoplethysmographic detection of the dorsal and palmar skin of human subjects. Both red and orange were able to detect, too; however, its higher wavelength, meant penetration in the next deeper level of the skin, which is dermis layer which already involved blood and

other vessels that absorbed light. The results further confirmed the fact that age and gender are relative to the amount of melanin present. For example in the 2g (41-year old female), 5g (10-year old female) and 6g (5-year old female) instances, particularly the four-yellow LEDs and phototransistor testing in the dorsal and palmar skin at Figures 9 and 13, a decline in the amount of reflected light meant greater absorbed light as a result of a higher amount of melanin present.

Among the quantities of LED tested, four pieces of yellow proved to offer the highest sensor response to all light detectors used. Phototransistor gave the highest sensor response among the detectors used and is the best detector to be used in this type of application.

## DISCLOSURES

The authors declare that there are no conflicts of interest in the conduct of this research.

## REFERENCES

- [1] J. Allen, **Photoplethysmography and its application in clinical physiological measurement**, *Physiological Measurement*, vol. 28, no. 3. 2007.
- [2] D. Castaneda, A. Esparza, M. Ghamari, C. Soltanpur, and H. Nazeran, **A review on wearable photoplethysmography sensors and their potential future applications in health care**, *International Journal of Biosensors & Bioelectronics*, vol. 4, no. 4. 2018.
- [3] Y. Yang, C. Liu, H. Yu, D. Shao, F. Tsow, and N. Tao, **Motion robust remote photoplethysmography in CIE Lab color space**, *Journal of Biomedical Optics*, vol. 21, no. 11. p. 117001, 2016.
- [4] M. Elgendi *et al.*, **The use of photoplethysmography for assessing hypertension** - *npj Digital Medicine*, *npj Digit. Med.*, vol. 2, no. 60, 2019.
- [5] T. Biedermann *et al.*, **The influence of stromal cells on the pigmentation of tissue-engineered dermo-epidermal skin grafts**, *Tissue Engineering - Part A*, vol. 21, no. 5–6. pp. 960–969, 2015.
- [6] A. N. Bashkatov *et al.*, **Optical properties of melanin in the skin and skinlike phantoms**, in *Proc. SPIE 4162 Controlling Tissue Optical Properties: Applications in Clinical Study*, 2000.
- [7] P.A.Riley, **Melanin** - *ScienceDirect*, *Int. J. Biochem. Cell Biol.*, vol. 29, no. 11, pp. 1235–1239, 1997.
- [8] S. Quinn, **Photoplethysmography - (IR Heart Rate Monitor): 5 Steps (with Pictures)**, *Instructables*, 2018. [Online]. Available: <https://www.instructables.com/id/Photoplethysmography-IR-Heart-Rate-Monitor/>. [Accessed: 15-Feb-2019].
- [9] Y.-C. Du and A. Stephanus, **The feasibility study of photoplethysmography features for arteriovenous fistula stenosis detection in hemodialysis patients with statistical approach** - *IEEE Conference Pu, IEEE Int. Conf. Appl. Syst. Invent.*, pp. 457–460, 2018.
- [10] L. Pu, P. J. Chacon, H. C. Wu, and J. W. Choi, **Novel tailoring algorithm for abrupt motion artifact**

- removal in photoplethysmogram signals**, *Biomedical Engineering Letters*, vol. 7, no. 4, pp. 299–304, 2017.
- [11] S. A. Shinde and P. Raja Rajeswari, **A novel hybrid framework for cuff-less blood pressure estimation based on vital bio signals processing using machine learning**, *Int. J. Adv. Trends Comput. Sci. Eng.*, vol. 9, no. 2, pp. 1556–1561, 2020.
- [12] A. Anil, R. Rajan, and R. Varghese, **Preliminary Medical Monitoring System in Ambulance for Rescue of Accident Victims**, pp. 1118–1121, 2019.
- [13] S. Usman and N. Harun, **Estimation of HbA1c Level Among Diabetic Patients using Second Derivative of Photoplethysmography**, 2017.
- [14] A. Morley, J. J. Davenport, M. Hickey, and J. P. Phillips, **Development and optimization of a miniaturized fiber-optic photoplethysmographic sensor**, *Optical Engineering*, vol. 56, no. 11, p. 1, 2017.
- [15] Z. Patel, M. A. Thaha, and P. A. Kyriacou, **Development of an intraluminal intestinal photoplethysmography sensor - IEEE Conference Publication, 2017 39th Annu. Int. Conf. IEEE Eng. Med. Biol. Soc.**, pp. 1840–1843, 2017.
- [16] C. M. Chen, R. Kwasnicki, B. Lo, and G. Z. Yang, **Wearable tissue oxygenation monitoring sensor and a forearm vascular phantom design for data validation**, *Proceedings - 11th International Conference on Wearable and Implantable Body Sensor Networks, BSN 2014*, pp. 64–68, 2014.
- [17] S. Tuna, M. R. Bozkurt, M. K. Ucar, and C. Bilgin, **Sleep staging using photoplethysmography signal and kNN nearest neighbor algorithm**, *2016 24th Signal Processing and Communication Application Conference (SIU)*, pp. 1373–1376, 2016.
- [18] R. A. Fathy, H. Wang, and L. Ren, **Comparison of UWB Doppler radar and camera based photoplethysmography in non-contact multiple heartbeats detection**, *BioWireless 2016 - Proceedings, 2016 IEEE Topical Conference on Biomedical Wireless Technologies, Networks, and Sensing Systems*, pp. 25–28, 2016.
- [19] D. Jarchi and A. J. Casson, **Estimation of heart rate from foot worn photoplethysmography sensors during fast bike exercise**, *Proceedings of the Annual International Conference of the IEEE Engineering in Medicine and Biology Society, EMBS*, vol. 2016-October, pp. 3155–3158, 2016.
- [20] H. Njoun and P. A. Kyriacou, **Photoplethysmography\_ Towards a non-invasive pressure measurement technique - IEEE Conference Publication, 2016 38th Annu. Int. Conf. IEEE Eng. Med. Biol. Soc.**, pp. 611–614, 2016.
- [21] S. S. Shahrabaki, B. Ahmed, T. Penzel, and D. Cvetkovic, **Photoplethysmography derivatives and pulse transit time in overnight blood pressure monitoring**, *Proceedings of the Annual International Conference of the IEEE Engineering in Medicine and Biology Society, EMBS*, vol. 2016-October, pp. 2855–2858, 2016.
- [22] D. Kurian, J. J. P.L., K. Radhakrishnan, and A. A. Balakrishnan, **Drowsiness Detection Using Photoplethysmography Signal - IEEE Conference Publication, 2014 Fourth Int. Conf. Adv. Comput. Commun.**, pp. 73–76, 2014.
- [23] S. Sone, T. Hayase, K. Funamoto, and A. Shirai, **Simultaneous analysis system for blood pressure and flow using photoplethysmography and ultrasonic-measurement-integrated simulation**, *Proceedings of the Annual International Conference of the IEEE Engineering in Medicine and Biology Society, EMBS*, pp. 1827–1830, 2013.
- [24] H. Haneishi, I. Nishidate, K. Nakano, K. Niizeki, Y. Aizu, and D. J. McDuff, **Evaluation of arterial oxygen saturation using RGB camera-based remote photoplethysmography**, p. 35, 2018.
- [25] Y. Sun, S. Hu, V. A. Peris, R. Kalawsky, and S. Greenwald, **(PDF) Noncontact imaging photoplethysmography to effectively access pulse rate variability**, *J. Biomed. Opt.*, vol. 18, no. 6, 2013.
- [26] C. I. Nwafor *et al.*, **Assessment of a noninvasive optical photoplethysmography imaging device with dynamic tissue phantom models**, *Journal of Biomedical Optics*, vol. 22, no. 09, p. 1, 2017.
- [27] M. Finžgar and P. Podržaj, **Feasibility of assessing ultra-short-term pulse rate variability from video recordings**, *PeerJ*, vol. 2020, no. 1, 2020.
- [28] S. Fallet, V. Moser, F. Braun, and J.-M. Vesin, **Imaging Photoplethysmography: What are the Best Locations on the Face to Estimate Heart Rate?**, *2016 Comput. Cardiol. Conf.*, 2016.
- [29] H. Demirezen and C. E. Erdem, **An overview of non-contact photoplethysmography**, *2017 25th Signal Process. Commun. Appl. Conf.*, pp. 1–4, 2017.
- [30] C. Ojeda, **Analysis on the Optical Response of Ldr and Phototransistor in Photoplethysmography - ScienceDirect**, *Sens. Bio-Sensing Res.*, vol. 28, no. 100334, 2020.
- [31] D. Barolet, **Light-Emitting Diodes (LEDs) in Dermatology**, *Semin. Cutan. Med. Surg.*, vol. 27, no. 4, pp. 227–38, 2009.
- [32] R. Sarkar and S. Bansal, **Skin pigmentation in relation to gender: truth and myth**, *Pigment International*, vol. 4, no. 1, p. 1, 2017.
- [33] M. D. Vasanop Vachimaron, **Pigmentary Changes Associated with Skin Aging**, *The Dermatologist*, vol. 19, no. 11, 2011.
- [34] L. Lindberg and P. Oberg, **Photoplethysmography. Part 2. Influence of light source wavelength**, *US Natl. Libr. Med. Natl. Institutes Heal.*, vol. 29, no. 1, pp. 48–54, 1991.
- [35] G. Baranoski and A. Krishnaswamy, **An introduction to light interaction with human skin**, *Rita*, vol. XI, no. 1, p. 56, 2004.
- [36] C. Farley, A. Kassu, S. Sadate, and A. Sharma, **Transmission of UV\_visible light through model human epidermis at varying ambient humidity**, in *Open Journal of Applied Sciences*, 2016, pp. 153–157.
- [37] M. Mallick and S. Ghosh, **Optical Property of Dermis**

- and Epidermis Layer**, *Int. J. Adv. Res. Sci. Eng.*, vol. 4, no. 11, pp. 282–287, 2015.
- [38] T. Igarashi, K. Nishino, and S. K. Nayar, **The appearance of human skin: A survey**, vol. 3, no. 1. 2007.
- [39] K. M. R. Tabal, **Nitrogen Deficiency Level Assessment Device for Rice (*Oryza sativa L.*)**, *Int. J. Adv. Trends Comput. Sci. Eng.*, vol. 9, no. 3, pp. 2834–2841, 2020.
- [40] C. Y. Wright, R. M. Lucas, T. Kapwata, Z. Kunene, and J. L. du Plessis, **Towards a reliable, non-invasive melanin assessment for pigmented skin**, *Ski. Res. Technol.*, vol. 25, no. 1, pp. 100–102, 2019.